Liquid Crystals
Publication details, including instructions for authors and subscription information:
http://www.informaworld.com/smpp/title~content=t713926090

Dielectric response and quasielastic light scattering on freely suspended films of the SmC * α phase in an external transverse electric field

M. Conradi; I. Muševič; M. ČepiČ

Online publication date: 11 November 2010

To cite this Article Conradi, M. , Muševič, I. and ČepiČ, M.(2002) 'Dielectric response and quasielastic light scattering on freely suspended films of the SmC * α phase in an external transverse electric field', Liquid Crystals, 29: 8, 1063 — 1072
To link to this Article: DOI: 10.1080/02678290210145229
URL: http://dx.doi.org/10.1080/02678290210145229

LIQUID CRYSTALS, 2002, VOL. 29, NO. 8, 1063–1072

Taylor & Francis
Taylor & Francis Group

Dielectric response and quasielastic light scattering on freely suspended films of the SmC^*_α phase in an external transverse electric field

M. CONRADI
J. Stefan Institute, Jamova 39, 1000 Ljubljana, Slovenia

I. MUŠEVIČ*
Faculty of Mathematics and Physics, University of Ljubljana, Jadranska 19, 1000 Ljubljana, Slovenia; and J. Stefan Institute, Jamova 39, 1000 Ljubljana, Slovenia

and M. ČEPIČ
Faculty of Education, University of Ljubljana, Kardeljeva ploščad 16, 1000 Ljubljana, Slovenia; and J. Stefan Institute, Jamova 39, 1000 Ljubljana, Slovenia

(*Received 23 January 2002; accepted 13 March 2002*)

A theoretical analysis of dynamic properties of freely suspended films of a SmC^*_α phase in an external electric field is performed within the 'clock' model, where the interactions up to next-nearest neighbours are considered. It is shown, that for an N-layer film, N amplitude and N phase fluctuation modes are present. The relaxation rates of the amplitude modes are in the MHz region, whereas the phase modes are typically in the kHz region. Magnitudes of the dielectric response and quasielastic light scattering cross-sections for individual modes are calculated as a function of an electric field applied along the smectic layers.

1. Introduction

There has been considerable and continuous interest in the structure of new phases formed by antiferroelectric liquid crystal materials since the discovery of the antiferroelectric SmC^*_α phase [1]. Various techniques, such as resonant X-ray scattering [2], dielectric spectroscopy [3, 4], optical rotation [5] and ellipsometry on bulk [6] and freely suspended films [7, 8], have been used to characterize the structure of the SmC^*_α and the two ferrielectric phases, SmC^*_{FI1} and SmC^*_{FI2}. The experimental evidence shows that the SmC^*_α phase is a tilted smectic phase, with a helical period that extends over typically ten smectic layers [2, 7] and it is therefore similar to the ferroelectric SmC* phase.

The structures of the SmC^*_α phase and the two ferrielectric phases, as well as the ferroelectric and antiferroelectric phases, are well described with the 'clock model' first developed by Čepič and Žekš [9]. This is a 3D-XY phenomenological model based on the idea of interlayer interactions that was first introduced by Sun and Orihara [10]. The model treats a system of N smectic layers as a set of individual smectic layers with their own phase transitions, which are thermodynamically coupled via interactions to the nearest and next-nearest neighbouring layers. Whereas the static properties of the SmC^*_α phase are rather well understood, little is known about the dynamics of freely suspended films and the interactions between the smectic layers that determine the structures. Recently, a study reported on the observed dynamics in antiferroelectric freely suspended films [11], where the oscillating electric field was applied in the smectic layers and the linear response was measured in the reflected light. The observed dynamics could be clearly attributed to the structure of the suspended film, but no detailed theoretical explanation was given.

In this paper, the dynamics of a finite system of N tilted and polar smectic layers is considered from the point of view of the eigendynamics of N coupled layers with $2N$ degrees of freedom. N degrees of freedom correspond to phase fluctuations and the remaining N

*Author for correspondence; e-mail: igor.musevic@ijs.si

Liquid Crystals ISSN 0267-8292 print/ISSN 1366-5855 online © 2002 Taylor & Francis Ltd
http://www.tandf.co.uk/journals
DOI: 10.1080/02678290210145229

degrees of freedom to the tilt magnitude fluctuations. We use a standard 'clock' model, discarding chiral interactions [9]. First, the equilibrium structures are obtained by minimizing the total free energy of the system of N coupled smectic layers, using a method first proposed by Rovšek *et al.* [12]. The excitation spectrum of such a system of N coupled smectic layers is then analysed by applying Landau–Khalatnikov equations of motion. We calculate the relaxational eigenvalues and eigenvectors of the fluctuations and follow the changes in the spectrum induced by the application of an external electric field. The calculations are presented for $N=6$ and $N=7$ smectic layers in the SmC^*_α phase. Based on the calculated eigenvectors, a dielectric response of a freely suspended film, as well as the quasielastic light scattering cross sections for different experimental geometries are calculated.

2. Static and dynamic properties of a SmC^*_α freely suspended film

We study here a freely suspended film of the SmC^*_α phase formed of N smectic layers. The molecular orientation within the i-th layer is described by the two-dimensional order parameter:

$$\xi_i = \vartheta_i(\cos\varphi_i, \sin\varphi_i). \tag{1}$$

Here, ϑ_i is the magnitude of the tilt angle and φ_i is the phase of the director in the i-th layer. The two dimensional order parameter ξ_i is within the xy-plane and the normal to the smectic planes is along the z-axis.

The stability of the structure of the SmC^*_α phase in an external d.c. electric field ($\mathbf{E}_{\text{d.c.}} = \mathbf{E}\ (0, 1, 0)$), which is applied in the y-direction, is analysed by expanding the free energy of a system of N coupled smectic layers in the most simple form:

$$G = \sum_{i=1}^{N} \frac{a_0}{2}\vartheta_i^2 + \frac{b_0}{4}\vartheta_i^4 + \frac{a_1}{2}[\vartheta_i\vartheta_{i+1}\cos(\varphi_i - \varphi_{i+1})] + \frac{a_2}{8}[\vartheta_i\vartheta_{i+2}\cos(\varphi_i - \varphi_{i+2})] - C\mathbf{E}\vartheta_i\cos\varphi_i. \tag{2}$$

The coefficients $a_0 = \alpha(T - T_0)$ and b_0 describe the intralayer interactions and to the largest extent determine the value of the tilt angle. The next two terms are the lowest order terms that describe the interactions between the neighbouring layers, whereas the last term describes the coupling of the spontaneous polarization of each layer, $\mathbf{P}_i = \vartheta_i(-\sin\varphi_i, \cos\varphi_i)$, with the external electric field. The surface interactions of the outer layers are implicitly taken into account if we define the order parameter $\xi_i = 0$ for $i < 1$ and $i > N$. This means that the two outer layers, as well as their first interior neighbours, interact only with the layers in the interior of the film, but there is no molecular interaction with empty space outside the film. Following the procedure of Rovšek *et al.* [12], we expand the free energy (2) by writing each component of the order parameters as a sum of its equilibrium value ξ_i^0 and a small correction $\delta\xi_i$:

$$\vartheta_i = \vartheta_i^0 + \delta\vartheta_i, \quad \varphi_i = \varphi_i^0 + \delta\varphi_i. \tag{3}$$

The expansion is performed up to the second order in corrections. Then, we obtain stationary values of the free energy by minimization with respect to small corrections of the tilt and phase in each layer:

$$\frac{\partial G}{\partial\vartheta_i} = 0, \quad \frac{\partial G}{\partial\varphi_i} = 0, \quad i = 1, \ldots N. \tag{4}$$

We obtain a system of coupled linear equations for the set of corrections $\delta\vartheta_i$ and $\delta\varphi_i$, which are solved separately [13] with an iterative numerical procedure. The initial approximation for the structure of the SmC^*_α phase at zero electric field is usually taken with some constant value of the tilt and the symmetric orientation of the phase through the set of layers. Then, we repeatedly improve the initial approximation for the structure until the resulting set of tilt and phase vectors satisfies a desired numerical precision. This two-stage iteration process is repeated at some higher value of the applied electric field and the new equilibrium structure is calculated in the same way as before by separately solving the set of equations for $\delta\vartheta_i$ and $\delta\varphi_i$.

As an example, we show in figures 1(*a*) and 2(*a*) the behaviour of a system with $N=6$ and $N=7$ layers in an external electric field applied perpendicularly to the layer normal. The values of the material parameters are $a_0/\alpha = -4$ K, $b_0/\alpha = 40$ K, $\alpha_2/\alpha = 2.5$ K, $\alpha = 4\times10^3$ J m^{-3} K^{-1}, $C = 1.5\times10^8$ V m^{-1} and $a_1/\alpha = -1.4$ K for $N=6$ and $a_1/\alpha = -1.6$ K for $N=7$ layers [6]. The values of a_0 and b_0 are chosen in such a way that they represent a SmC^*_α phase at a temperature 4 K below the SmA phase. The ratio of a_1 and a_2 is chosen so that it represents a SmC^*_α phase with a period of approximately 6 and 7 layers, respectively. At zero field, the molecular arrangement is already asymmetric, as the phase angles of the surface layers are different from those in the interior. The tilt magnitudes are close to 19 degrees for both systems with $N=6$ and $N=7$ layers and are also slightly different for the outer layers [14]. This is due to the absence of intermolecular interactions between the surface layers and the empty space outside the film.

As one can expect, by increasing the field strength the molecules tend to align in the plane perpendicular to the field, as the electric dipoles are preferentially aligned into the field direction. At some value of the critical field $\mathbf{E}_c$, the short helix SmC^*_α structure is unwound and we

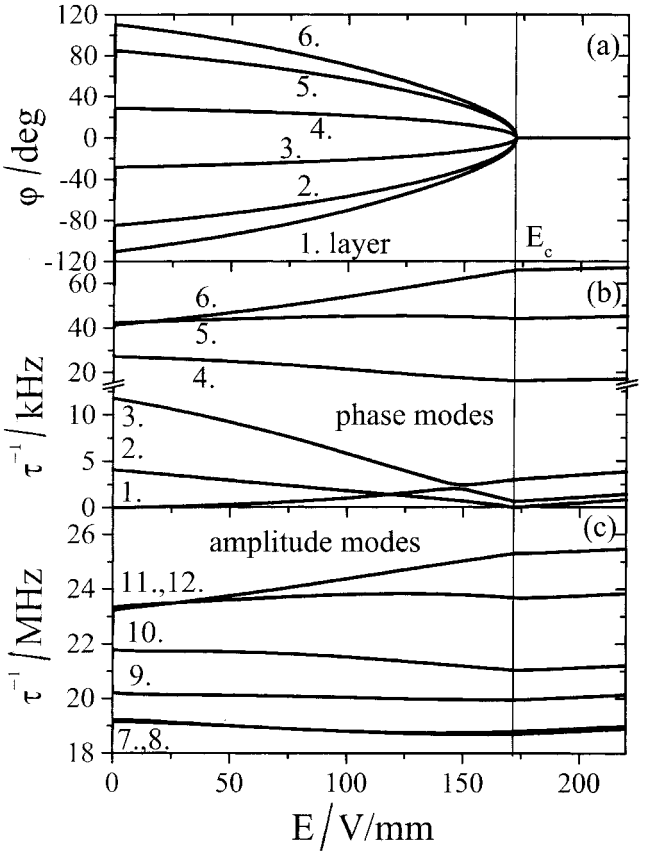

Figure 1. (*a*) The phase angle of the tilt direction in each layer of a 6-layer system as a function of external field. (*b*) Relaxation rates of six phase-fluctuation modes and (*c*) relaxation rates of six tilt-fluctuation modes in a 6-layer system as a function of the electric field. The values of the material parameters are: $a_0/\alpha = -4$ K, $b_0/\alpha = 40$ K, $\alpha_1/\alpha = -1.4$, K, $\alpha_2/\alpha = 2.5$ K, $\alpha = 4.10^3$ J m^{-3} K^{-1}, $C = 1.5 \times 10^8$ V m^{-1} [6].

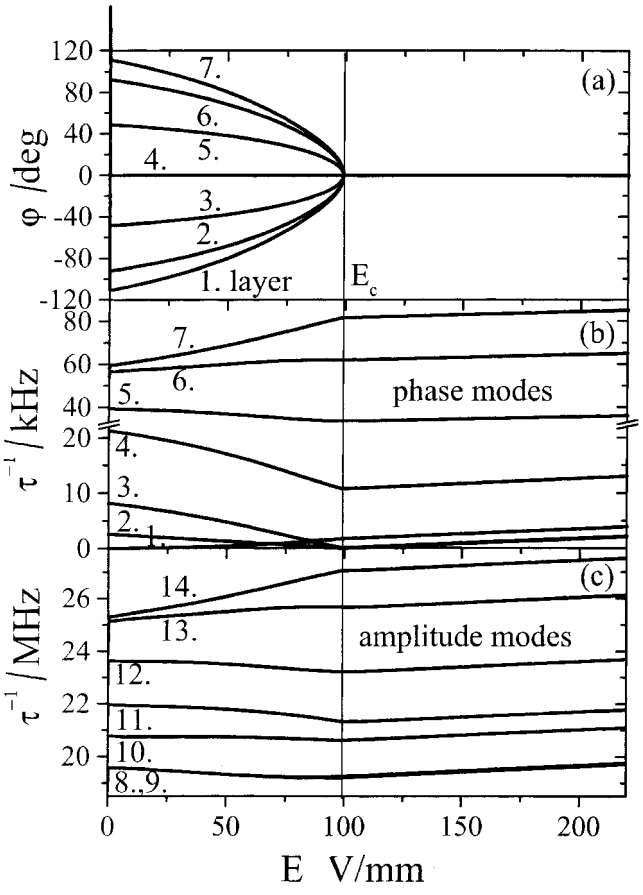

Figure 2. (*a*) The phase angle of the tilt direction in each layer of a 7-layer film as a function of external electric field along the smectic layers. (*b*) Relaxation rates of seven phase modes in a 7-layer system and (*c*) relaxation rates of seven tilt-fluctuation modes. The values of the material parameters are: $a_0/\alpha = -4$ K, $b_0/\alpha = 40$ K, $\alpha_1/\alpha = -1.67$ K, $\alpha_2/\alpha = 2.5$ K, $\alpha = 4 \times 10^3$ J m^{-3} K^{-1}, $C = 1.5 \times 10^8$ V m^{-1} [6].

have a uniformly aligned and unwound $\mathrm{Sm\tilde{C}^*_\alpha}$ phase. The unwinding transition is similar to the very well known unwinding of the helicoidal ferroelectric SmC* phase in a transverse electric field [15]. The values of the critical electric field $\mathbf{E}_c$ for this transition depend strongly on the value of the piezoelectric constant C, describing the bilinear coupling between the polarization and the tilt. This constant is of the order of 10^6 V m^{-1} in the ferroelectric liquid crystal DOBAMBC [15], which has a spontaneous polarization $\mathbf{P}_s = 3 \times 10^{-5}$ A s m^{-2}. As the spontaneous polarization of most materials that form the SmC^*_α phase is typically 100 times larger, we choose a larger value of $C \sim 10^8$ V m^{-1}. This results in critical electric fields of the order $\mathbf{E}_c \sim 170$ V mm^{-1} for $N = 6$ and $\mathbf{E}_c \sim 100$ V mm^{-1} for $N = 7$ layers which are definitely within experimental reach. The decrease of the value of the critical field with increasing number of layers is an indication of a crossover between a finite system and the bulk.

One also notices that the field-induced transition into the unwound phase is continuous for $N = 6$ and $N = 7$ smectic layers, and for this range of free energy parameters the phase of each smectic layer continuously merges to zero.

For the analysis of the dynamical properties of the SmC^*_α phase, we use the well known Landau–Khalatnikov formalism, which describes the regression of a given fluctuation of the order parameter ξ towards equilibrium:

$$-\gamma \frac{\mathrm{d}\xi}{\mathrm{d}t} = \frac{\partial G}{\partial \xi} \tag{5}$$

where, γ is the rotational viscosity coefficient and $\partial G/\partial \xi$ is a thermodynamic restoring force that drives the system back to equilibrium. Here we consider only the fluctuations with the wave vector along the layer normal,

whereas there is no component of the fluctuations along the smectic layers. We write the order parameter in each layer as a sum of the equilibrium value and a small deviation similar to equation (3). We search for the time dependent solution of equation (5) of the form

$$\delta\xi = \xi^0 \exp(-t/\tau_j) \tag{6}$$

where ξ^0 is a general N-dimensional eigenvector and τ_j is the corresponding relaxation time. The system of Landau–Khalatnikov differential equations is then transformed into the eigenvalue problem for the fluctuations of an N-layer film [13]:

$$\left(\boldsymbol{D} + \frac{\gamma}{\tau_j}\boldsymbol{I}\right) \boldsymbol{\Psi}^j = 0. \tag{7}$$

Here, $\boldsymbol{\Psi}$ is a $2N$-dimensional fluctuation vector corresponding to the eigenmode τ_j^{-1}. The first N components represent the fluctuations of the magnitude (i.e. amplitudons) and the rest of the N components represent the fluctuations of the phase of the tilt (i.e. phasons):

$$\boldsymbol{\Psi}_i^j = (\delta\vartheta_i, \delta\varphi_i)$$

where i is the index of the layer and goes from 1 to N. The dynamical matrix $\boldsymbol{D}$ represents the coefficients of the linearized set of equations $\partial G/\partial \boldsymbol{\Psi}^j$ in a $2N \times 2N$-dimensional matrix form [15] and $\boldsymbol{I}$ is the identity matrix.

For an N-layer film we have therefore $2N$ degrees of freedom and we thus obtain $2N$ eigenvalues τ_j^{-1} and $2N$ corresponding eigenvectors $\boldsymbol{\Psi}^j$. Each eigenvalue represents a distinct relaxation rate of a distinct fluctuation of a coupled system of N smectic layers. However, in most cases (such as sufficiently low temperature), the coupling between the magnitude and the phase can be neglected and we obtain two independent sets of modes: pure amplitude fluctuation and pure phase fluctuation modes. The corresponding fluctuations of the magnitude and the phase of the tilt in the i-th layer can be determined from the components of the calculated eigenvector.

Further on, we will only be interested in phase fluctuation modes, since the contribution of the amplitude fluctuation modes to the dielectric response and quasielastic scattering is negligible compared with that of the phase fluctuation modes.

We show in figures 1(*b*) and 2(*b*) two examples of the calculated phase relaxation rates in an external electric field for $N = 6$ and $N = 7$-layer systems, respectively. As one can expect, the electric field breaks the continuous rotational symmetry of a free space and the system of N smectic layers can no longer freely rotate around the normal to the smectic layers. As a result, we expect that the Goldstone, zero frequency mode—the 1st mode in figures 1(*b*) and 2(*b*)—would no longer exist. This is indeed reflected in the spectrum of fluctuations for finite field which clearly shows that even the lowest frequency mode gains a finite relaxation rate in a field and a finite frequency gap appears in the spectrum. The frequency gap is of the order of several kHz close to the critical field. The modes therefore become 'massive' in an external applied electric field.

Particular attention has to be paid also to the mode representing the critical fluctuation that condenses and is responsible for the phase transition into the unwound SmC_α^* phase. This is the 2nd phase mode in figures 1(*b*) and 2(*b*). Looking at the symmetry properties of the corresponding fluctuation vector, we see that it represents a coherent molecular movement that tries to constrain the molecules in the x-direction and the dipoles in the y-direction. Its relaxation rate indeed goes to zero at the critical field, as expected from this simple symmetry argument.

After the critical field has been reached, the relaxation rates of all modes grow linearly with the magnitude of the applied field. This is consistent with perfect alignment of the electric dipoles of the molecules of the liquid crystal into the direction of the applied field.

3. Dielectric response of a freely suspended film of a SmC_α^* phase

The dielectric response is studied within the Landau–Khalatnikov dynamical response to the small, time oscillating electric field which is applied in addition to the static electric field in a freely suspended film of SmC_α^* phase:

$$\mathbf{E}_\omega = \mathbf{E}_0(0, 1, 0)\exp(\mathrm{i}\omega t). \tag{8}$$

Here, $\omega = 2\pi\nu$, where ν is the frequency of the measuring electric field. The coupling between the oscillating electric field $\mathbf{E}_\omega$ and the electric polarization of each smectic layer gives an additional contribution to the free energy of the system (2):

$$G_{\mathbf{E}_\omega} = -\mathbf{E}_\omega \ \mathbf{P} = -C\mathbf{E}_0\vartheta_i\cos\varphi_i\exp(\mathrm{i}\omega t). \tag{9}$$

The increase of the free energy due to the fluctuations can now be written as a sum of the free energy of the system in a static electric field (2) and the free energy due to the additional oscillating electric field (9):

$$\Delta G = \boldsymbol{\Psi}^+ \boldsymbol{D}\boldsymbol{\Psi} + \mathbf{U}\boldsymbol{\Psi}. \tag{10}$$

Here $\boldsymbol{\Psi}$ is a $2N$-dimensional vector representing the fluctuations of the amplitude and the phase in each layer, as defined in the previous chapter, and the matrix $\boldsymbol{D}$ is a $2N \times 2N$-dimensional dynamical matrix as defined in equation (7). $\mathbf{U}$ is a $2N$-dimensional vector representing an additional contribution due to the oscillating electric field in each layer:

$$\mathbf{U} = C\mathbf{E}_0(0, \vartheta_i\cos\varphi_i)\exp(\mathrm{i}\omega t).$$

The solution of the Landau–Khalatnik kinetic equation (5) is, in the case of an additional oscillating field, of the form:

$$\boldsymbol{\Psi} = \boldsymbol{\Psi}_0 \exp(\mathrm{i}\omega t). \tag{11}$$

Equation (10) is then transformed into an inhomogeneous eigenvalue problem for the unknown $\boldsymbol{\Psi}_0$

$$(2\boldsymbol{D} + \mathrm{i}\omega\gamma\boldsymbol{I})\ \boldsymbol{\Psi}_0 = \mathbf{U}. \tag{12}$$

It is solved with a standard mathematical procedure giving a linear response of the system to the oscillating electric field of the form:

$$\boldsymbol{\Psi}_0 = \sum_{j=1}^{N} \frac{1}{\tau_j^{-1} + \mathrm{i}\omega} \frac{\boldsymbol{\Psi}^{j+}\ \mathbf{U}}{|\boldsymbol{\Psi}^j|^2}\ \boldsymbol{\Psi}^j. \tag{13}$$

Here, τ_j^{-1} is the relaxation rate of the j-th eigenmode and $\boldsymbol{\Psi}^j$ is the corresponding eigenmode fluctuation.

As one can expect, the linear response is directly related to the interaction of the system with an additional oscillating electric field and is determined with the scalar product $\boldsymbol{\Psi}^{j+}\ \mathbf{U}$ in equation (13). As a result, a given electric field excites only the modes with a finite value of this scalar product. Physically, this means that it couples only the fluctuation modes that carry some electric polarization along the external measuring electric field. Only these modes contribute to the dielectric response.

The polarity of a particular eigenmode can be estimated from the symmetry properties of its eigenvectors. For 6 and 7-layer films we find that there are three phase modes with the electric polarization along the external field. Figures 3 and 4 show the symmetries of these modes in zero electric field. The symmetry of the first modes in figures 3 (*a*) and 4 (*a*) correspond to the previously defined critical mode, leading to the phase transition to the

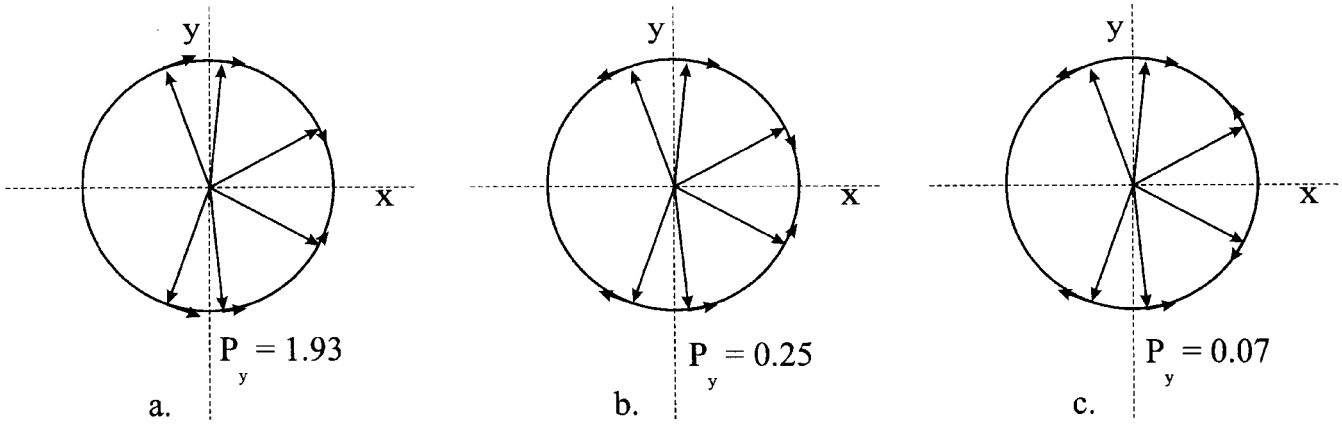

Figure 3. The eigenvectors of the phase modes that contribute to the dielectric response in a 6-layer film at zero electric field. The small arrows indicate the direction of the fluctuation of the molecules in each of the six layers. The rest of the modes carry electric polarization along the *x*-axis.

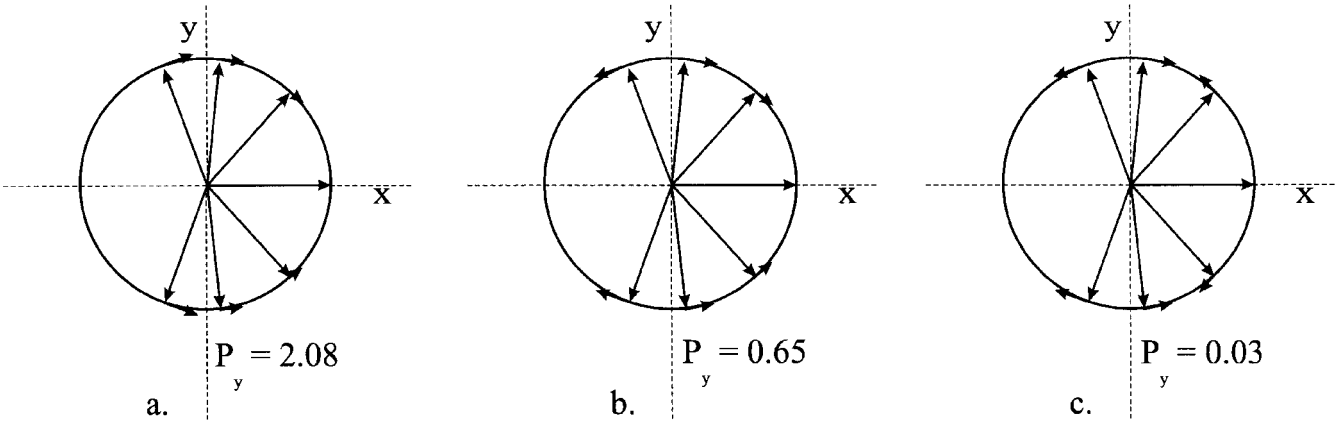

Figure 4. The eigenvectors of the phase modes that contribute to the dielectric response in a 7-layer film at zero electric field. The small arrows indicate the direction of the fluctuation of the molecules in each of the seven layers. The rest of the modes carry electric polarization along the *x*-axis.

unwound phase. This mode is characterized by rotation of molecules in pairs in opposite directions. The second and third mode represent an in-plane movement of the molecules in the outer layers, figures 3(*b*), 3(*c*) and 4(*b*), 4(*c*).

For each mode the magnitude of the induced polarization was calculated. This is a measure of the electric susceptibility of the system:

$$\chi_{\mathbf{E}} = \frac{\delta \mathbf{P}}{\delta \mathbf{E}_\omega} = \frac{\sum_{i=1}^{N} \delta[\vartheta_i(-\sin\varphi_i, \cos\varphi_i)]}{\delta \mathbf{E}_\omega}. \qquad (14)$$

Here i counts for the number of layers. In our case only the component of the induced polarization parallel to the electric field is non-zero, which makes the susceptibility a scalar:

$$\chi_{\mathbf{E}} = \chi_{yy} = \frac{\delta \mathbf{P}_y}{\delta \mathbf{E}_0} = C \sum_{i=1}^{N} \delta\varphi_{i0} \quad \vartheta_i(-\sin\varphi_i). \qquad (15)$$

Here, we considered only the contribution due to the phase fluctuations, $\delta\varphi_{i0}$, since the amplitude fluctuations, $\delta\vartheta_{i0}$, give around a 1000-times smaller contribution to the dielectric constant.

In figures 5 and 6 we present the behaviour of the static dielectric constant calculated for each polar phase mode in the external static electric field for $N = 6$ and $N = 7$ layers, respectively. The static dielectric constant of the critical mode increases in the vicinity of the critical field, but there is no divergence characteristic for bulk systems, curves 5(*a*) and 6(*a*). The dielectric constants of the next two modes drop continuously to one at the critical field, curves 5(*b*) and 6(*b*). However, the polarity of the modes in figures 3(*c*) and 4(*c*) is so small compared with the modes in figures 3(*a*, *b*) and 4(*a*, *b*) that dielectric response is hardly observed on the scale in curves 5(*b*) and 6(*b*).

In figure 7 we present the frequency dispersion of the real $\varepsilon'(\omega)$ and imaginary part $\varepsilon''(\omega)$ of the dielectric response in the 6-layer system in zero d.c. electric field. For the phase fluctuation modes, the relaxation process was analysed with the Cole–Cole equation for the complex dielectric response:

$$\varepsilon(\omega) = \varepsilon(\infty) + \sum_{j=1}^{N} \frac{\varepsilon_j(\omega = 0) - \varepsilon(\infty)}{1 + \mathrm{i}\omega\tau_j} \qquad (16)$$

where $\varepsilon(\infty)$ is the high frequency limit value of the dielectric constant, τ_j is the relaxational time corresponding to each phase fluctuation mode and $\varepsilon_j(\omega = 0)$ is the static value of the dielectric constant for each mode. As one can expect, three relaxation processes, that correspond to the phase fluctuations shown in figures 3(*a*, *b c*) are observed.

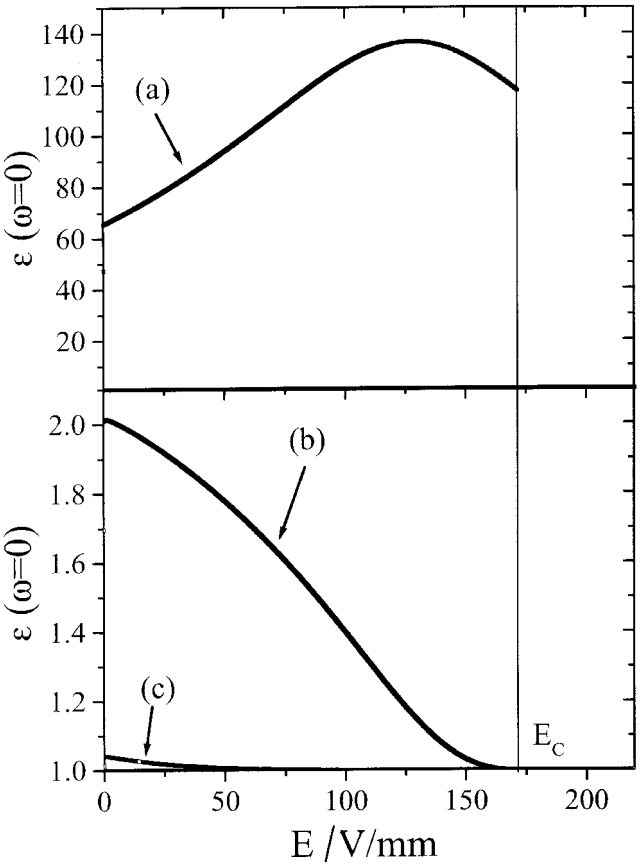

Figure 5. Contributions of the individual modes to the dielectric constant of an $N = 6$ layer system. The modes (*a*), (*b*) and (*c*) are the same as those in figure 3. The values of the material parameters are: $a_0/\alpha = -4$ K, $b_0/\alpha = 40$ K, $\alpha_1/\alpha = -1.4$ K, $\alpha_2/\alpha = 2.5$ K, $\alpha = 4 \times 10^3$ J m^{-3} K^{-1}, $C = 1.5 \times 10^8$ V m^{-1} [6].

4. Quasielastic light scattering of a freely suspended film of a SmC^*_α phase

Whereas modes carrying electric polarization in the direction perpendicular to the direction of the external electric field are invisible in the dielectric response experiments, they may become visible in a quasielastic light scattering experiment. Here, each fluctuation mode represents local reorientation of the molecular long axis. This reorientation represents a disturbance in the local dielectric tensor that results in a quasielastic scattering of light. This scattering is strong in liquid crystals due to the large optical birefringence and large thermally induced reorientations of the direction of the local optical axis. They induce a small perturbation $\delta\underline{\varepsilon}$ in the optical dielectric constant $\underline{\varepsilon}$:

$$\underline{\varepsilon}(\mathbf{r}, t) = \underline{\varepsilon}(0) + \delta\varepsilon(\mathbf{r}, t). \qquad (17)$$

Here, $\underline{\varepsilon}(0)$ denotes the time and space averaged dielectric tensor of a SmC^*_α phase and $\delta\underline{\varepsilon}$ can be expressed in terms of amplitude and phase fluctuation modes in each

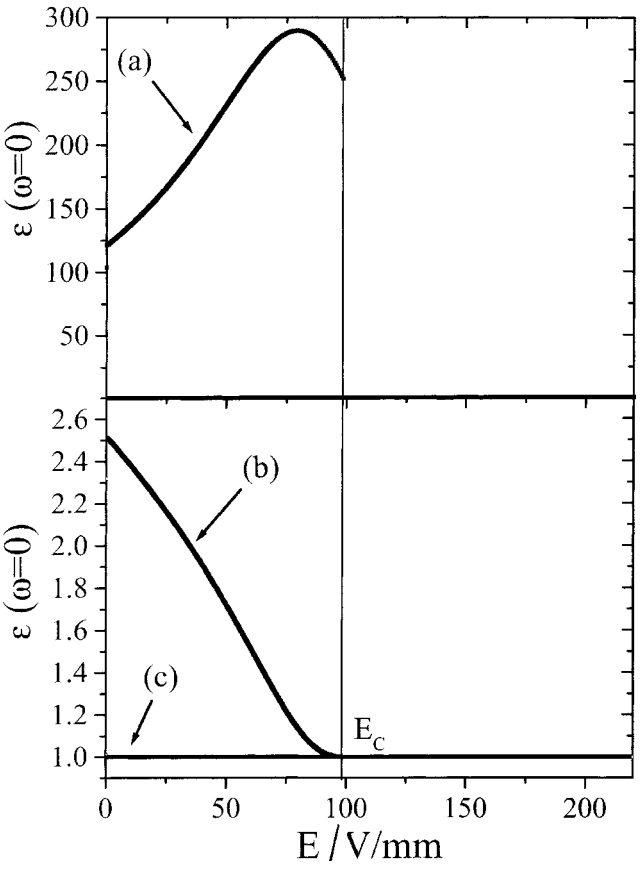

Figure 6. Contributions of the individual modes to the dielectric constant of an $N = 7$ layer system. The modes (*a*), (*b*) and (*c*) are the same as those in figure 4. The values of the material parameters are: $a_0/\alpha = -4$ K, $b_0/\alpha = 40$ K, $\alpha_1/\alpha = -1.67$ K, $\alpha_2/\alpha = 2.5$ K, $\alpha = 4 \times 10^3$ J m^{-3} K^{-1}, $C = 1.5 \times 10^8$ V m^{-1} [6].

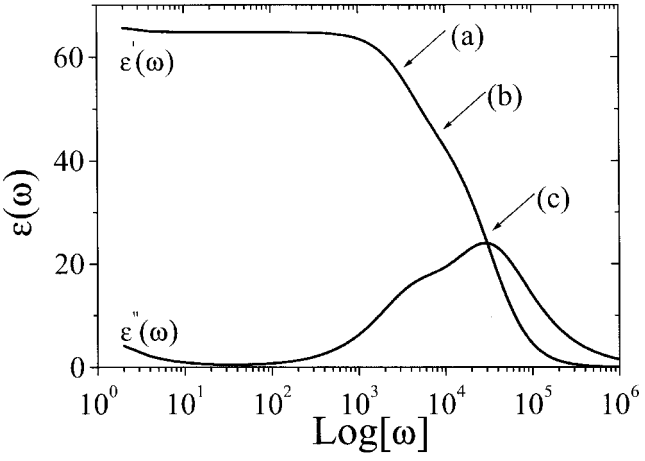

Figure 7. Real and imaginary parts of the dielectric response in the 6-layer system in zero d.c. electric field. (*a*), (*b*) and (*c*) denote the three relaxation processes corresponding to the phase mode fluctuations in figures 3 (*a*, *b*, *c*). The frequencies of the modes are 4, 27 and 40 kHz, respectively.

layer [15]:

$$\delta\varepsilon = (\varepsilon_3 - \varepsilon_1)\begin{pmatrix} 0 & 0 & \cos\varphi_i \\ 0 & 0 & \sin\varphi_i \\ \cos\varphi_i & \sin\varphi_i & 0 \end{pmatrix}\delta\vartheta_i + (\varepsilon_3 - \varepsilon_1)\begin{pmatrix} 0 & 0 & -\sin\varphi_i \\ 0 & 0 & \cos\varphi_i \\ -\sin\varphi_i & \cos\varphi_i & 0 \end{pmatrix}\delta\varphi_i. \tag{18}$$

Here, φ_i represents the equilibrium phase angle in each layer and $\delta\vartheta_i$ and $\delta\varphi_i$ represent the amplitudon and phason excitatons.

In a light scattering process, the incident light with wave vector $\mathbf{k}_i$ and polarization **i** (which can be either σ or π) is scattered on a thermal fluctuation $\delta\underline{\varepsilon}$ (17) into a light wave with wave vector $\mathbf{k}_f$ and polarization **f**, which can also be either σ or π. Following the standard approach [17] to the scattering process, we find that the amplitude of the scattered electric field at a distance R from the sample is proportional to the Fourier transform of the disturbance of the dielectric tensor $\delta\underline{\varepsilon}$ (17):

$$\mathbf{E}_s(\mathbf{R}, t) = \frac{-|\mathbf{k}_f|^2 \mathbf{E}_0}{4\pi R\varepsilon_0} \exp[\mathrm{i}(\mathbf{k}_f R - \omega t)]\langle\delta\underline{\varepsilon}_{if}(\mathbf{q}_s, t)\rangle \tag{19}$$

$\langle\delta\underline{\varepsilon}_{if}(\mathbf{q}_s, t)\rangle$ is the Fourier transform of the fluctuating part of the dielectric tensor, projected onto the vector of the polarization of the incoming (**i**) and the scattered (**f**) light, respectively, at the scattering wave vector $\mathbf{q}_s = \mathbf{k}_i - \mathbf{k}_f$. In view of the small thickness of the sample, d, it is equal to the space averaged dielectric tensor along the z-axis:

$$\langle\delta\underline{\varepsilon}_{if}(\mathbf{q}_s, t)\rangle = \int \mathrm{d}z[\mathbf{f}\ \ \delta\underline{\varepsilon}(z, t)\ \ \mathbf{i}]\exp(\mathrm{i}\mathbf{q}_s z) = \exp(\mathrm{i}\mathbf{q}_s d)\mathbf{f}\ \ \langle\delta\underline{\varepsilon}(\mathbf{q}_s, t)\rangle_d\ \ \mathbf{i}. \tag{20}$$

In a light scattering experiment, the time autocorrelation function of the scattered light intensity $I(t)$ is detected:

$$G^{(2)}(\tau) = \langle I(0)I(t)\rangle = \lim_{T\to\infty}\frac{1}{T}\int_0^T \mathrm{d}t I(t)I(t+\tau). \tag{21}$$

In the case of the heterodyne regime, the autocorrelation function $G^{(2)}(\tau)$ (19) is proportional to the autocorrelation function of the Fourier component of the dielectric tensor field [15]:

$$G^{(2)}(\tau) \sim Re\{\langle\delta\underline{\varepsilon}_{if}(\mathbf{q}_s, 0)\underline{\varepsilon}^*_{if}(\mathbf{q}_s, \tau)\rangle\}. \tag{22}$$

Since the fluctuations of the dielectric tensor $\delta\underline{\varepsilon}_{if}(\mathbf{q}_s, \tau)$ are directly proportional to the amplitude and the phase mode fluctuations (17), measurement of the time-autocorrelation function of the scattered light intensity directly reflects the dynamic of the order parameter.

In the light scattering experiment, the polarizations of the incident and the scattered beam determine the contributions of different modes to the light scattering signal. The scattering amplitudes were calculated for the case of scattering of π polarized light: $\mathbf{i} = (\sin\alpha, 0, -\cos\alpha)$ into σ polarized light: $\mathbf{f} = (0, 1, 0)$, where α is the angle between the wave vector of the incident light and the z-axis (figure 8):

$$\mathbf{f}\ \delta\varepsilon\ \mathbf{i} \sim (0, 1, 0)\ \delta\underline{\varepsilon} \begin{pmatrix} \sin\alpha \\ 0 \\ -\cos\alpha \end{pmatrix}$$

$$= \cos\alpha \sum_{i=1}^{N} (\varepsilon_3 - \varepsilon_1)\ (\cos\varphi_i \delta\varphi_i + \sin\varphi_i \delta\vartheta_i). \quad (23)$$

The scattering amplitude is in this geometry proportional to both the phase and the amplitude fluctuations. The signal is most intense for $\alpha = 0$. We also see that for this scattering geometry only the modes that carry no electric polarization along the external d.c. field participate in the scattering process.

In figures 9 and 10 we present the scattering amplitudes only for the phase fluctuations $\delta\varphi_i$. Figures 9 (*a*, *b*) and 10 (*a*, *b*) present the two modes that make significant contribution to the light scattering amplitudes shown in figures 9 (*c*) and 10 (*c*). From the symmetries of the fluctuation vectors we see that the incident light is most intensely scattered by the Goldstone mode fluctuations, figures 9 (*a*), 10 (*a*). The corresponding scattering amplitude diverges in zero electric field. As the electric field increases, the scattering amplitude decreases, which is consistent with breaking of the rotational symmetry of the system.

An interesting cross-over is observed close to the critical electric field in figures 9 and 10. The two most intense modes here 'exchange' their cross-sections. An analysis of the eigenvectors shows that these two modes indeed also exchange the symmetry of their eigenvectors, which is related to the cross-over of their relaxation rates, as indicated in figures 1 (*b*) and 2 (*b*).

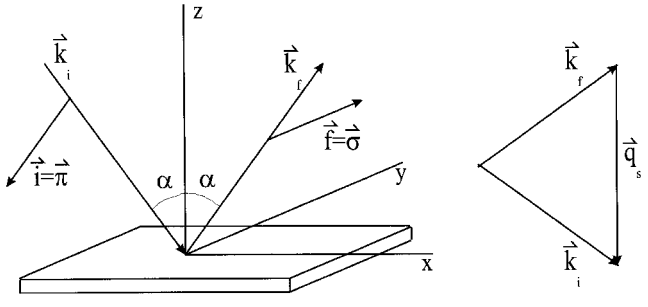

Figure 8. A typical geometry for the study of light scattering. **i** and **f** are polarizations of incident and scattered light.

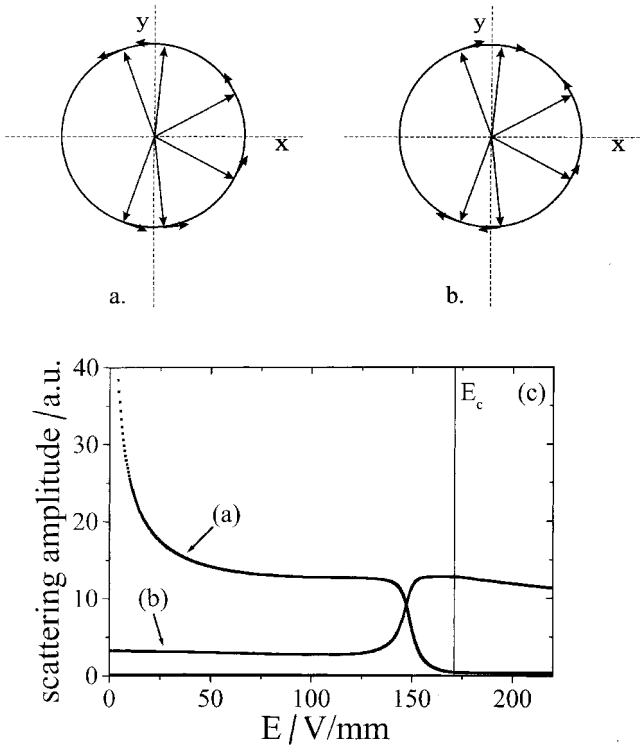

Figure 9. (*a*) and (*b*): the eigenvectors of the two non-polar modes contributing significantly to the light scattering process. (*c*) Scattering amplitudes for $N = 6$ layers for the case of a π–σ scattering process. The values of the material parameters are: $a_0/\alpha = -4$ K, $b_0/\alpha = 40$ K, $\alpha_1/\alpha = -1.4$ K, $\alpha_2/\alpha = 2.5$ K, $\alpha = 4 \times 10^3$ J m^{-3} K^{-1}, $C = 1.5 \times 10^8$ V m^{-1} [6].

As an example of another scattering geometry, we show in figure 11 the scattering amplitudes for the phase fluctuations of an $N = 6$-layer film for the scattering process of π polarized light: $\mathbf{i} = (\sin\alpha, 0, -\cos\alpha)$ into π polarized light: $\mathbf{f} = (\sin\beta, 0, -\cos\beta)$. α and β are here the angles between the z-axis and the incident and scattered light, respectively. The calculated scattering amplitude is in this experiment proportional to:

$$\mathbf{f}\ \delta\varepsilon\ \mathbf{i} = \sin(\alpha + \beta) \sum_{i=1}^{N} (\varepsilon_3 - \varepsilon_1)$$

$$(-\sin\varphi_i \delta\varphi_i + \cos\varphi_i \delta\vartheta_i). \quad (24)$$

Here, the signal is most intense for the angle $\alpha + \beta = \pi/2$. For this scattering geometry we find that the modes carrying electric polarization along the d.c. field contribute to the scattering process. The main contribution corresponds to the critical mode shown in figure 3 (*a*).

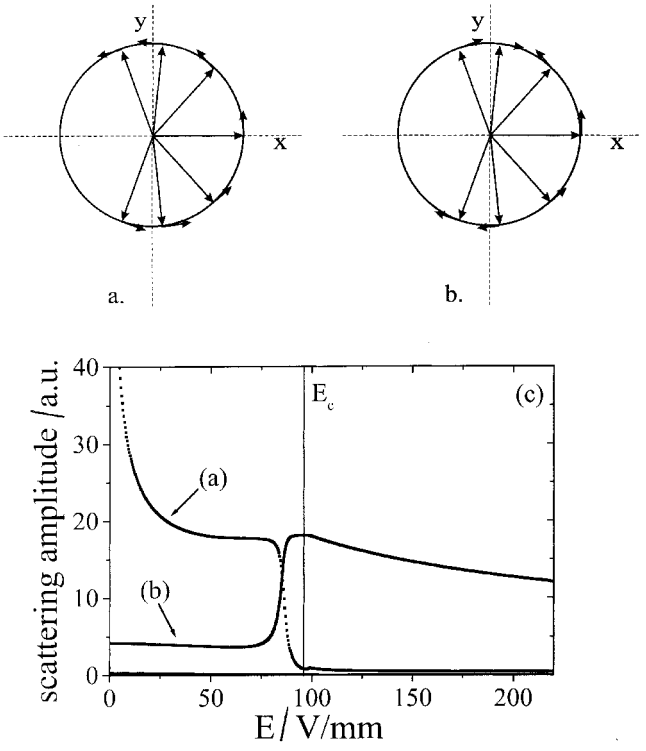

Figure 10. (*a*) and (*b*): the eigenvectors of the two non-polar modes contributing significantly to the light scattering process. (*c*) Scattering amplitudes for $N = 7$ layers for the case of a π–σ scattering geometry. The values of the material parameters are: $a_0/\alpha = -4$ K, $b_0/\alpha = 40$ K, $\alpha_1/\alpha = -1.67$ K, $\alpha_2/\alpha = 2.5$ K, $\alpha = 4 \times 10^3$ J m^{-3} K^{-1}, $C = 1.5 \times 10^8$ V m^{-1} [6].

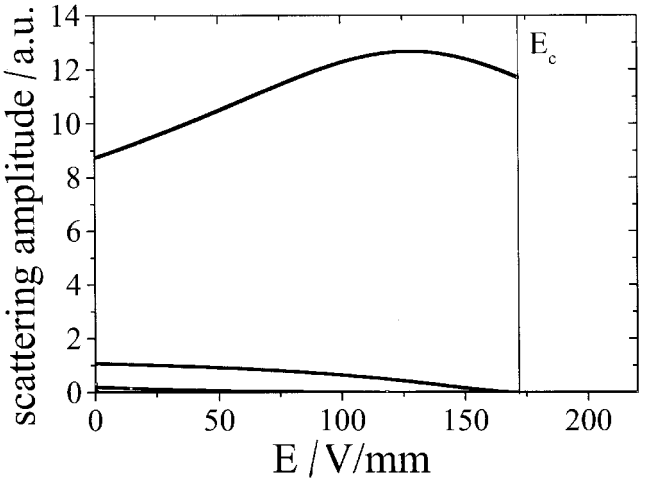

Figure 11. Scattering amplitudes for $N = 6$ layers for the case of a π–π scattering geometry. The values of the material parameters are: $a_0/\alpha = -4$ K, $b_0/\alpha = 40$ K, $\alpha_1/\alpha = -1.4$ K, $\alpha_2/\alpha = 2.5$ K, $\alpha = 4 \times 10^3$ J m^{-3} K^{-1}, $C = 1.5 \times 10^8$ V m^{-1} [6].

5. Conclusions

In conclusion, we have presented a theoretical analysis of the dielectric and the quasielastic light scattering properties of a freely suspended film of the SmC$^*_\alpha$ phase in an external static electric field, applied in the plane of the smectic layers. Using realistic values of the free energy parameters, we have shown that the critical electric field for the unwinding of the SmC$^*_\alpha$ phase in freely suspended films depends on the number of layers and is experimentally accessible. We studied the dynamical properties of the thin film system using the Landau–Khalatnikov formalism and calculated relaxational eigenvalues and corresponding eigenvectors of the fluctuations. We have shown, that for an N-layer film, we obtain N phase modes and N amplitude modes, the latter being nearly a 1000-times less intense. Furthermore, we have shown that in an external d.c. electric field, the phase modes can be grouped into two groups. The first group of modes carries fluctuating polarization along the external field; the other group has fluctuating electric polarization in a perpendicular direction.

From the symmetry properties of the fluctuations, we were able to deduce the contributions of individual modes to the linear dielectric response or light scattering cross-section. The dielectric response to the oscillating electric field is significant for modes, carrying some electric polarization along the external measuring field. On the contrary, in the light scattering experiment, the contributions of different modes to the signal can be selected by choosing proper polarizations of the incident and scattered beam. Whereas in the light scattering experiment the magnitude of the detected scattered signal seems non-problematic, the magnitude of the capacitance of the thin film system is extremely low. For a 10 nm–1 μm thick film, it is estimated to be 10^{-2}–10^{-4} pF, which is impossible to measure using a standard bridge technique. However, a linear electro-optic response technique could easily be used, in this case giving direct optical access to dielectrically active modes.

References

[1] Chandani, A. D. L., Ouchi, Y., Takezoe, H., and Fukuda, A., 1988, *Jpn. J. appl. Phys.*, **27,** L276.

[2] Mach, P., Pindak, R., Levelut, A. M., Barois, P., Nguyen, H. T., Huang, C. C., and Furenlid, L., 1998, *Phys. Rev. Lett.*, **81,** 1015.

[3] Hiraoka, K., Taguchi, A., Ouchi, Y., Takezoe, H., and Fukuda, A., 1990, *Jpn. J. appl. Phys.*, **29,** L103.

[4] Hou, J., Schacht, J., Giesselmann, F., and Zugenmaier, P., 1997, *Liq. Cryst.*, **22,** 409.

[5] Muševič, I., and Škarabot, M., 2001, *Phys. Rev. E*, **64,** 051706.

[6] Škarabot, M., Čepič, M., Žekš, B., Blinc, R., Heppke, G., Kityk, A. V., and Muševič, I., 1998, *Phys. Rev. E*, **58,** 575.

[7] Schlauf, D., and Bahr, Ch., 1999, *Phys. Rev. E*, **60,** 6816.
[8] Olson, D. A., Pankratz, S., Johnson, P. M., Cady, A., Nguyen, H. T., and Huang, C. C., 2001, *Phys. Rev. E*, **64,** 061711.
[9] Čepič, M., and Žekš, B., 1995, *Mol. Cryst. liq. Cryst.*, **263,** 61; Roy, A., and Madhusudana, N. V., 1996, *Europhys. Lett.*, **36,** 221; Lorman, V. L., Bulbitch, A. A., and Toledano, P., 1994, *Phys. Rev. E*, **49,** 1367.
[10] Sun, H., Orihara, H., and Ishibashi, Y., 1991, *J. phys. Soc. Jpn.*, **60,** 4175.
[11] Yasuyuki, K., Noriyuki, K., and Reinosuke, H., 2001, *Phys. Rev. E*, **64,** 011703.
[12] Rovšek, B., Čepič, M., and Žekš, B., 2000, *Ferroelectrics*, **244,** 67.
[13] Conradi, M., Muševič, I., and Čepič, M., submitted to *Physical Review E*.
[14] Fera, A., Optiz, R., de Jeu, W. H., Ostrovskii, B. I., Schlauf, D., and Bahr, Ch., 2001, *Phys. Rev. E*, **64,** 021702.
[15] Muševič, I., Blinc, R., and Žekš, B., 2000, *The Physics of Ferroelectric and Antiferroelectric Liquid Crystals* (Singapore: World Scientific).
[16] Kutnjak-Urbanc, B., 1990, MsC thesis, University of Ljubljana.
[17] Berne, B. J., and Pecora, R., 1976, *Dynamic Light Scattering* (New York: John Wiley and Sons, Inc.).